ACCOUNTS
of chemical research

C–H Bond Activation by Oxygen-Centered Radicals over Atomic Clusters

XUN-LEI DING,[†] XIAO-NAN WU,[†,‡] YAN-XIA ZHAO,[†] AND SHENG-GUI HE*,[†]

[†]*Beijing National Laboratory for Molecular Sciences, State Key Laboratory for Structural Chemistry of Unstable and Stable Species, Institute of Chemistry, Chinese Academy of Sciences, Beijing 100190, P. R. China, and* [‡]*Graduate School of Chinese Academy of Sciences, Beijing 100039, P. R. China*

RECEIVED ON MAY 14, 2011

CONSPECTUS

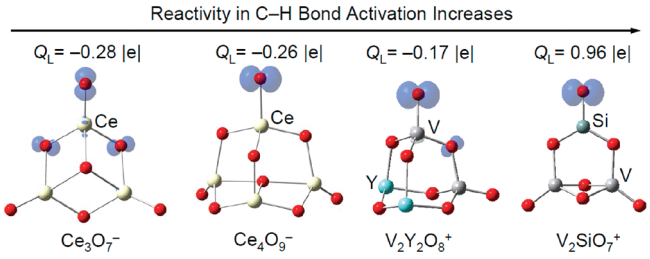

Saturated hydrocarbons, or alkanes, are major constituents of natural gas and oil. Directly transforming alkanes into more complex organic compounds is a value-adding process, but the task is very difficult to achieve, especially at low temperature. Alkanes can react at high temperature, but these reactions (with oxygen, for example) are difficult to control and usually proceed to carbon dioxide and water, the thermodynamically stable byproducts. Consequently, a great deal of research effort has been focused on generating and studying chemical entities that are able to react with alkanes or efficiently activate C–H bonds at lower temperatures, preferably room temperature.

To identify low-temperature methods of C–H bond activation, researchers have investigated free radicals, that is, species with open-shell electronic structures. Oxygen-centered radicals are typical of the open-shell species that naturally occur in atmospheric, chemical, and biological systems. In this Account, we survey atomic clusters that contain oxygen-centered radicals ($O^{-\bullet}$), with an emphasis on radical generation and reaction with alkanes near room temperature. Atomic clusters are an intermediate state of matter, situated between isolated atoms and condensed-phase materials. Atomic clusters containing the $O^{-\bullet}$ moiety have generated promising results for low-temperature C–H bond activation.

After a brief introduction to the experimental methods and the compositions of atomic clusters that contain $O^{-\bullet}$ radicals, we focus on two important factors that can dramatically influence C–H bond activation. The first factor is spin. The $O^{-\bullet}$-containing clusters have unpaired spin density distributions over the oxygen atoms. We show that the nature of the unpaired spin density distribution, such as localization and delocalization within the clusters, heavily influences the reactivity of $O^{-\bullet}$ radicals in C–H bond activation.

The second factor is charge. The $O^{-\bullet}$-containing clusters can be negatively charged, positively charged, or neutral overall. We discuss how the charge state may influence C–H bond activation. Moreover, for a given charge state, such as the cationic state, it can be demonstrated that local charge distribution around the $O^{-\bullet}$ centers can also significantly change the reactivity in C–H bond activation. Through judicious synthetic choices, spin and charge can be readily controllable physical quantities in atomic clusters. The adjustment of these two properties can impact C–H bond activation, thus constituting an important consideration in the rational design of catalysts for practical alkane transformations.

1. Introduction

Direct transformation of saturated hydrocarbons (alkanes), which are major constituents of natural gas and oil, into more valuable products is a difficult problem that has attracted interests of researchers from most of the disciplines within chemistry.[1−5] Activation of the carbon–hydrogen (C–H) bond is an essential step in alkane transformation because a saturated hydrocarbon molecule will

Published on the Web 10/21/2011 www.pubs.acs.org/accounts
10.1021/ar2001364

first see, or interact with, a reacting substrate only through the strong and localized C−H bonds that are usually chemically inert at low temperature.

Free radicals or species with open shell electronic structures can be highly reactive. It is possible to activate the very stable C−H bonds by radical species[6] at low or relatively low temperature, which may serve as a first step to solve serious problems that would occur in the transformation of alkanes at high temperature. Note that high temperature processes involved with alkanes usually result in low product selectivity, primary formation of thermodynamically stable byproducts carbon dioxide and water (as in combustion), and other related problems of economics and environment.[1]

Oxygen-centered radicals are typical of the open-shell species that naturally occur in atmospheric, chemical, and biological systems. Gas-phase studies have well characterized that the simplest oxygen radical, the free O^- anion ($O^{-\bullet}$), can react with the most stable saturated hydrocarbon molecule, methane (CH_4), through reaction 1 at room temperature with the first order rate constant $k_1 = 8.8 \times 10^{-11}$ cm^3 molecule^{-1} s^{-1}:[7]

$$O^{-\bullet} + CH_4 \rightarrow OH^- + CH_3 \qquad \Delta H_{0K} = -0.29\ \text{eV} \qquad (1)$$

Several condensed-phase studies proposed that $O^{-\bullet}$ radicals over oxide surfaces are important intermediates in selective oxidation of alkanes such as methane.[8−10] Due to the complexity of condensed phase systems, the structure−property relationship in the reactions of alkanes with the surface $O^{-\bullet}$ species is far from clear.

Atomic clusters are an intermediate state of matter situated between isolated atoms and condensed phase materials and can be studied under isolated, controlled, and reproducible conditions.[11] Many atomic clusters have been reported to contain $O^{-\bullet}$ centers.[12−16] In this Account, a detailed structure−property relationship for C−H activation by $O^{-\bullet}$ radicals is demonstrated and discussed based on the investigations of atomic clusters.

2. Methods

Oxide cluster ions are generated by laser ablation and reacted with small molecules in a fast flow reactor for about 60 μs under instantaneous total gas pressure around 200−300 Pa and carrier gas temperature about 300−400 K in our experiments. The product and unreacted reactant cluster ions enter into a time-of-flight (TOF) mass spectrometer for mass and intensity measurements. The first-order rate constant (k_1) for reaction of clusters with reactant molecules in the fast flow reactor is estimated by eq 2 below:

$$k_1 = \ln(I_0/I)/(\rho \Delta t) \qquad (2)$$

where I and I_0 are signal magnitudes of the clusters in the presence and absence of reactant gas, respectively; ρ is the molecular density of reactant gas, and Δt is the reaction time. Details on the experiments and density functional theory (DFT) calculations that are employed to study the structures and reaction mechanisms for cluster systems of interest are described in our previous publications.[16−19]

3. Compositions of Atomic Clusters with $O^{-\bullet}$ Radicals

Transition metal oxides (TMOs) including lanthanide oxides are extensively used catalyst materials in practice and study of TMO clusters is important to understand elementary reactions over TMO surfaces at a molecular level. We have recently proposed that it is useful to define a value (Δ) for an oxide cluster $M_xO_y^q$ to clarify the oxygen-richness or poorness:[16]

$$\Delta \equiv 2y - nx + q \qquad (3)$$

in which q is the charge number and n counts the highest oxidation state of element M. Scandium (Sc, [Ar]3d^{1}4s^2, $n = 3$) and cerium (Ce, [Xe]4f^{1}5d^{1}6s^2, $n = 4$) are the first d-block and the first f-block metals, respectively. Figure 1 shows that the least oxygen-rich ($\Delta = 1$) clusters $Sc_2O_4^-$, $Sc_4O_6^+$, $Ce_3O_7^-$, and $Ce_4O_9^-$ have very similar unpaired spin density (UPSD) distributions as the free O^- anion does: UPSD values of about 1μ_B are distributed in one or more oxygen 2p orbitals.[16,19,20] As a result, each of these clusters contains one or equivalently one unit of $O^{-\bullet}$ radical. In addition to the examples shown in Figure 1b,c, the DFT calculations indicate that for most of the early transition metals, the oxide clusters $M_xO_y^q$ ($x = 1-3$) with $\Delta = 1$ all contain $O^{-\bullet}$ radicals. These metals include groups 3−7 and 3d−5d elements except Cr and Mn, for which the $\Delta = 1$ clusters such as $(CrO_3)_{1-3}^+$ and $Mn_2O_7^+$ are species with unbroken O−O bonds and thus have no $O^{-\bullet}$ centers.[16] Figure 1d indicates that more oxygen-rich clusters ($\Delta > 1$) such as $Sc_3O_6^-$ ($\Delta = 2$) and $Sc_3O_7^-$ ($\Delta = 4$) may also contain $O^{-\bullet}$ radicals. The $Sc_3O_6^-$ cluster is a biradical that contains two $O^{-\bullet}$ centers, while both $O^{-\bullet}$ (mononuclear oxygen-centered radical) and $O_2^{-\bullet}$ (superoxide radical) exist in $Sc_3O_7^-$.

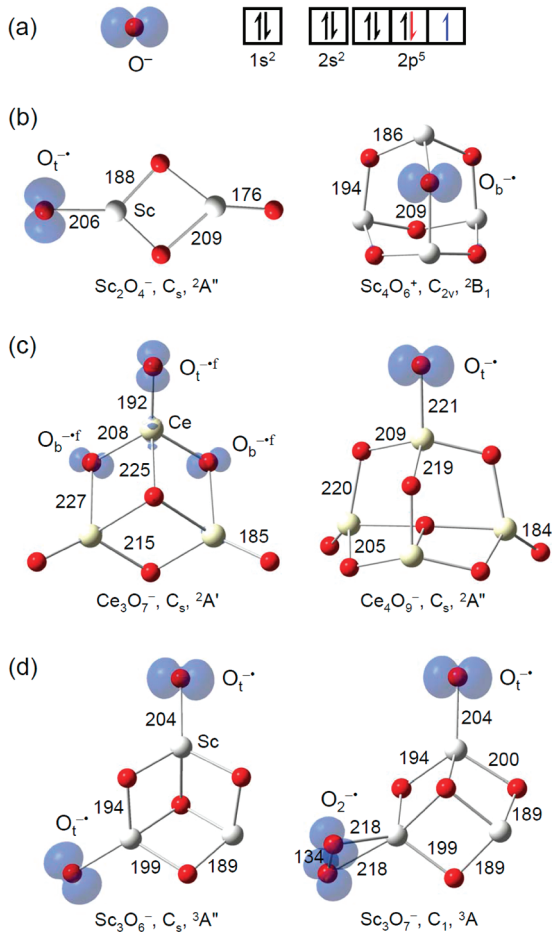

FIGURE 1. B3LYP/TZVP/SDD calculated profiles of unpaired spin density distributions for the free O^- anion (a) and selected scandium and cerium oxide clusters (b–d).[16,19,20] Bond lengths in this figure and all others throughout this Account are given in pm.

The oxygen atoms in the clusters with UPSDs close to $1\mu_B$ can be denoted as $O^{-\bullet}$, while those with a fraction of $1\mu_B$ (as in $Ce_3O_7^-$ shown in Figure 1c) may be denoted as $O^{-\bullet f}$. Furthermore, subscripts t and b ($O_t^{-\bullet}$, $O_b^{-\bullet}$; $O_t^{-\bullet f}$, $O_b^{-\bullet f}$) can be used to label the terminally and bridgingly bonded oxygen atoms, respectively. Figure 1b indicates that the $M-O_t^{-\bullet}$ or $M-O_b^{-\bullet}$ bond in each cluster is significantly longer than the normal $M=O_t$ double or $M-O_b$ single bond, respectively. For example, the $Sc-O_t^{-\bullet}$ bond in $Sc_2O_4^-$ is longer than $Sc=O_t$ by 30 pm. The $O^{-\bullet}$ centers with elongated $M-O^{-\bullet}$ bonds and locally open shell electronic structures can be active sites in the reactions with small molecules.

The DFT calculations suggest that hydrogen atom abstraction (HAA) reactions as described by reaction 1 over all of the $\Delta = 1$ clusters listed in Figure 2 are exothermic. For group 3 metals (Sc, Y, La), the HAA is less exothermic over the cationic clusters than anionic ones. In contrast, the HAA are much more exothermic over cations than anions for group 4–7 metal systems.

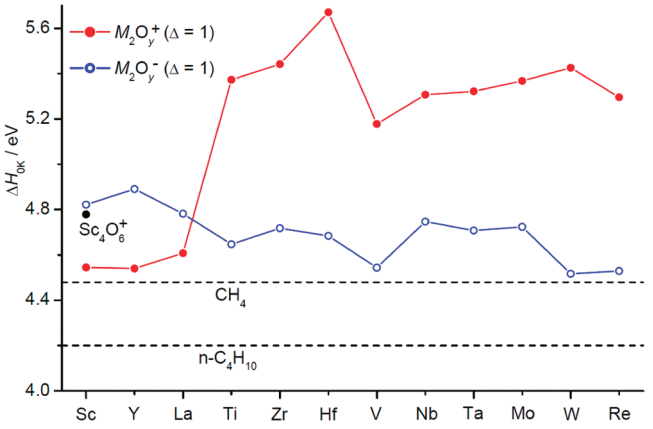

FIGURE 2. B3LYP/TZVP/Def2-TZVP calculated O–H bond energies of $M_2O_yH^{\pm}$ and $Sc_4O_6H^+$ clusters in which the compositions of $M_2O_y^{\pm}$ satisfy $\Delta = 1$ (see eq 3 in the text).[16] The C–H bond energies of methane and *n*-butane are indicated for comparison.

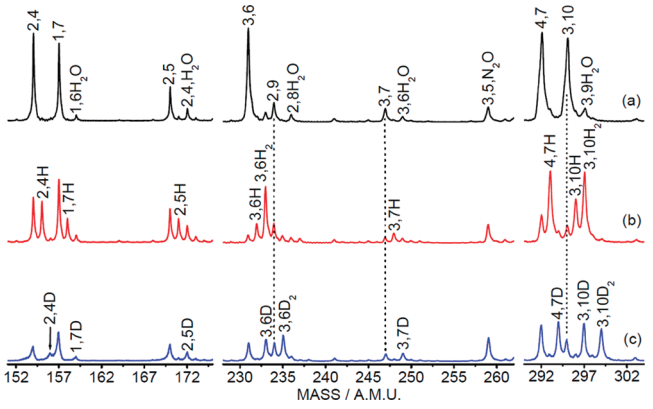

FIGURE 3. TOF mass spectra for reactions of $Sc_xO_y^-$ with He (a, for reference), 0.6 Pa *n*-C_4H_{10} (b), and 0.6 Pa *n*-C_4D_{10} (c). The $Sc_xO_y^-$ and $Sc_xO_yX^-$ (X = H, D, etc.) clusters are denoted as *x*,*y* and *x*,*y*X, respectively.

4. C–H Activation over Homonuclear Oxide Clusters

4.1. Oxide Clusters of Early Transition Metals. Figure 3 indicates that hydrogen atom pickup products that are due to both $\Delta = 1$ ($Sc_2O_4^-$ and $Sc_4O_7^-$) and $\Delta > 1$ (ScO_7^-, $Sc_2O_5^-$, and $Sc_3O_{6,7,10}^-$) clusters are generated in the reactions of $Sc_xO_y^-$ with *n*-butane in the fast flow reactor under near room temperature conditions. The estimated rate constants $k_1(Sc_2O_4^- + C_4H_{10})$, $k_1(Sc_3O_6^- + C_4H_{10})$, and $k_1(Sc_4O_7^- + C_4H_{10})$ are 8.0×10^{-11}, 2.9×10^{-10}, and 1.6×10^{-10} cm^3 $molecule^{-1}$ s^{-1}, respectively. A value of kinetic isotope effect $k_1(Sc_3O_6^- + C_4H_{10})/k_1(Sc_3O_6^- + C_4D_{10}) = 1.9$ can also be determined.[19]

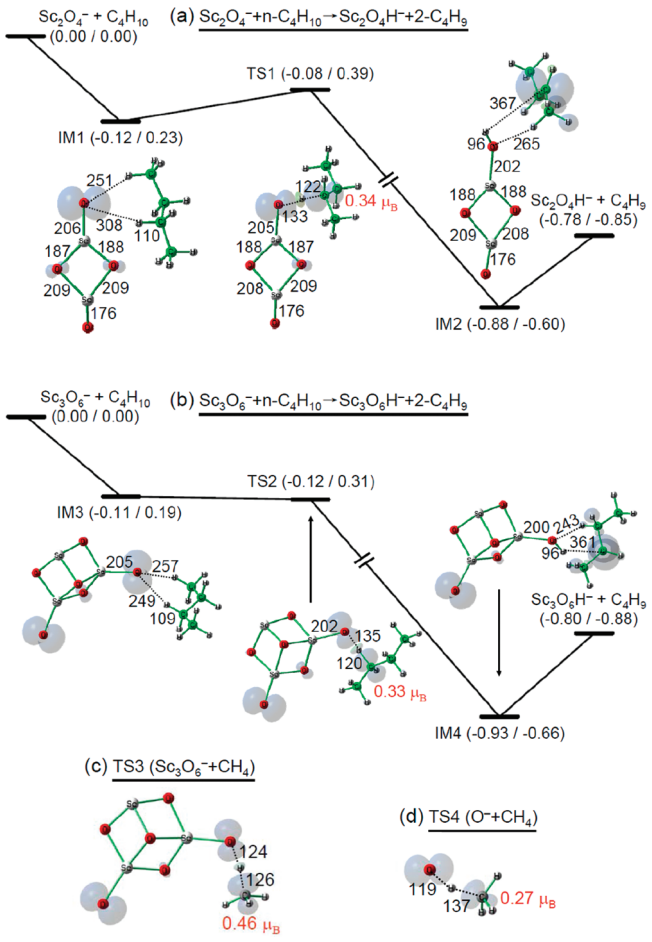

FIGURE 4. B3LYP/TZVP calculated potential energy profiles for reactions of n-C_4H_{10} with $Sc_2O_4^-$ (a) and $Sc_3O_6^-$ (b). The DFT calculated transition state structures for reactions of CH_4 with $Sc_3O_6^-$ cluster and O^- anion are given for comparison (c, d). The energies in eV are given in the parentheses as ($\Delta H_{0K}/\Delta G_{298K}$). Unpaired spin density values over related carbon atoms in the transition states are given.

Figure 4 plots the DFT calculated potential energy profiles for reactions 4 and 5 below:

$$Sc_2O_4^- + n\text{-}C_4H_{10} \rightarrow Sc_2O_4H^- + 2\text{-}C_4H_9 \qquad \Delta H_{0K} = -0.78\ \text{eV} \qquad (4)$$

$$Sc_3O_6^- + n\text{-}C_4H_{10} \rightarrow Sc_3O_6H^- + 2\text{-}C_4H_9 \qquad \Delta H_{0K} = -0.80\ \text{eV} \qquad (5)$$

It is apparent that the $O^{-\bullet}$ radicals over the reactant clusters are active sites that interact and react directly with the C–H bonds. The structures of the remaining part of the clusters such as the Sc_2O_3 moiety in $Sc_2O_4^-$ system (Figure 4a) change very slightly in the reactions.

The $Sc_3O_6^-$ cluster is a biradical and one $O^{-\bullet}$ radical is left in the product cluster $Sc_3O_6H^-$ that further reacts with a second n-C_4H_{10} to produce the double-hydrogen-atom pickup product $Sc_3O_6H_2^-$ (Figure 3). The characterization of $Sc_3O_6^-$ as an $O^{-\bullet}$ biradical rather than a peroxide species (O_2^{2-}) is further confirmed by photoelectron spectroscopy.[19] Figure 3 shows that $Sc_3O_{10}^-$ ($\Delta = 10$) has very similar reactivity as $Sc_3O_6^-$ does, suggesting that $Sc_3O_{10}^-$ is also a biradical although this requires further verification. Condensed phase studies proposed that surface $O^{-\bullet}$ radicals may be coupled to form $O^{-\bullet}\cdots O^{-\bullet}$ dimers, but it is difficult to characterize them.[21] The $Sc_3O_6^-$ cluster ions that can be isolated for detailed study may serve as an ideal model system to understand related surface chemistry of the $O^{-\bullet}\cdots O^{-\bullet}$ dimers.

The $\Delta = 4$ cluster $Sc_3O_7^-$ can also abstract a hydrogen atom from n-butane (Figure 3), which is in agreement with the DFT prediction that there is one $O^{-\bullet}$ center in this cluster (Figure 1d). The analysis of the structures of $Sc_3O_5^-$ (singlet, see Figure S1, Supporting Information) and $Sc_3O_7^-$ (triplet) suggests an important way of generating the highly reactive $O^{-\bullet}$ centers from less reactive species in metal oxides:

$$O^{2-}(\text{lattice oxygen}) + O_2 \rightarrow O^{-\bullet} + O_2^{-\bullet} \qquad (6)$$

The same mechanism also exists in $La_3O_5^- + O_2$,[22] $Zr_2O_6^- + O_2$,[23] $Nb_2O_5 + O_2$,[15] and $Ta_2O_5 + O_2$[15] cluster systems.

The free O^- anion reacts with methane (reaction 1) at room temperature with $k_1(O^- + CH_4) = 8.8 \times 10^{-11}$ cm^3 molecule^{-1} s^{-1},[7] while there is no evidence of methane activation by any of the cluster anions in Figure 3a ($k_1 < 10^{-13}$ cm^3 molecule^{-1} s^{-1}). The DFT calculated transition state energy (ΔH_{0K}, Figure 4c) for reaction 7 is 0.11 eV with respect to the separated reactants:

$$Sc_3O_6^- + CH_4 \rightarrow Sc_3O_6H^- + CH_3 \qquad \Delta H_{0K} = -0.44\ \text{eV} \qquad (7)$$

The $k_1(Sc_3O_6^- + CH_4)$ is estimated to be 4.9×10^{-14} cm^3 molecule^{-1} s^{-1} by using the experimentally determined $k_1(Sc_3O_6^- + C_4H_{10})$ and DFT calculated relative energetics.[19] This means that the nature of C–H activation by atoms (free $O^{-\bullet}$) and atomic clusters (ligated $O^{-\bullet}$) can be fundamentally different.

The HAA (reaction 1, 4, 5, or 7) involves transfers of one electron (e^-) and one proton (p^+) from the hydrocarbon molecule to the reacting $O^{-\bullet}$ atom.[24,25] Figure 4 indicates that the UPSDs of $0.46\mu_B$ from the reacting O atom have been transferred and redistributed over the C atom in TS3, while in TS4 the transferred and redistributed UPSDs are only $0.27\mu_B$, and most of the UPSDs ($\sim 0.73\mu_B$) are still

located over the O atom. This means that more electron transfer (ET) has taken place in TS3 than in TS4. In addition, the transferring H atom (denoted as **H**) is closer to the O atom in TS4 (d_{O-H} = 119 pm, free OH bond length is 97 pm) than in TS3 (d_{O-H} = 124 pm), while it is closer to the C atom in TS3 (d_{C-H} = 126 pm, free methane bond length is 109 pm) than in TS4 (d_{C-H} = 137 pm). This means that more proton transfer has taken place in TS4 than in TS3. Population analysis (Figure S2, Supporting Information) shows that for the $Sc_3O_6^-$+CH_4 reaction system, the natural charges on H_3C**H**, **H**, and H_3C moieties always increase (ET to Sc_3O_6 moiety) when **H** approaches the cluster. The amount of ET from H_3C**H** to Sc_3O_6 is 0.15|e| when the internal reaction coordinate (IRC) changes from −1.5 au (d_{O-H} = 165 pm) to 0.0 au (TS3, d_{O-H} = 124 pm). In contrast, the natural charge on H_3C**H** for the O^- + CH_4 system changes only slightly, and the net ET (0.02|e|) is from O to H_3C**H** in the IRC range of −1.5 au (d_{O-H} = 164 pm) to 0.0 au (TS4, d_{O-H} = 119 pm). The charge change on **H** for O^- + CH_4 is also very small (0.03|e| for IRC = −1.5 to 0.0 au). As a result, one may conclude that C−H activation by free $O^{-\bullet}$ radicals in vacuum (reaction 1) is a typical radical (H•) abstraction, while the C−H activation by the ligated $O^{-\bullet}$ radicals over atomic clusters (reaction 7, as well as reactions 4 and 5) is primarily characterized by ET.

The above nature of C−H activation over atomic clusters (ET) suggests that *$O^{-\bullet}$-containing cluster cations are more reactive than $O^{-\bullet}$-containing cluster anions* under the conditions that other related issues such as bond energies and UPSD distributions are similar. Our experimental study of the reactivity of early TMO cluster cations has identified HAA from methane by a series of Δ = 1 clusters: $(TiO_2)_{1-5}^+$, $(ZrO_2)_{1-4}^+$, $(HfO_2)_{1-2}^+$, $(V_2O_5)_{1-5}^+$, $(Nb_2O_5)_{1-3}^+$, $(Ta_2O_5)_{1-2}^+$, $(MoO_3)_{1-2}^+$, $(WO_3)_{1-3}^+$, and $Re_2O_7^+$.[26] The determined rate constants of $M_2O_y^+$ (Δ = 1) with CH_4 in our experiments are in the same order of magnitude (~10^{-10} cm^3 molecule^{-1} s^{-1}). Note that methane activation by $V_4O_{10}^+$ and a few MO_y^+ systems is identified by other independent studies.[3,27,28]

The HAA from methane by group 3 metal species such as $Sc_2O_3^+$, $Y_2O_3^+$, $La_2O_3^+$, and $Sc_4O_6^+$ is only slightly exothermic (Figure 2), in agreement with the result that the HAA from methane by these clusters is not identified in our experiments.[26] The HAA from less stable alkane molecules, n-butane by $Sc_2O_3^+$ and $Sc_4O_6^+$ clusters, can be observed and the experimentally estimated k_1-($Sc_2O_3^+$+C_4H_{10}) and k_1($Sc_4O_6^+$+C_4H_{10}) are 2.6 × 10^{-11} and 1.7 × 10^{-10} cm^3 molecule^{-1} s^{-1}, respectively. The much higher reactivity of $Sc_4O_6^+$ over $Sc_2O_3^+$ is consistent with the thermodynamics below:

$$Sc_2O_3^+ + n\text{-}C_4H_{10} \rightarrow Sc_2O_3H^+ + 2\text{-}C_4H_9 \qquad \Delta H_{0K} = -0.50\ \text{eV} \tag{8}$$

$$Sc_4O_6^+ + n\text{-}C_4H_{10} \rightarrow Sc_4O_6H^+ + 2\text{-}C_4H_9 \qquad \Delta H_{0K} = -0.74\ \text{eV} \tag{9}$$

Furthermore, the UPSDs in $Sc_2O_3^+$ (Figure S1, Supporting Information) are delocalized, while they are highly localized in $Sc_4O_6^+$. For the UPSD delocalized system $Sc_2O_3^+$, which has two $O_b^{-\bullet f}$ centers, the electronic and geometric structures involved with the additional $O_b^{-\bullet f}$ atom have to be properly reorganized in the HAA that finally forms a close shell product, $Sc_2O_3H^+$. The structure reorganization[24] can result in less favorable thermkinetics: higher HAA barrier or less steep reaction potential energy surface. More examples will be illustrated below to indicate that *UPSD localization versus delocalization* (termed as *local spin effect* in this Account) is a very important issue in the C−H activation by the $O^{-\bullet}$-containing clusters.

4.2. Cerium Oxide Clusters. Figures 1c and Figure S4a, Supporting Information, indicate that for cerium oxide cluster anions with Δ = 1, the UPSDs are delocalized in small clusters and become localized as the cluster size increases. The $Ce_3O_7^-$, $Ce_4O_9^-$, and $Ce_5O_{11}^-$ clusters contain $O_t^{-\bullet f}$, $O_t^{-\bullet}$, and $O_b^{-\bullet}$ radicals, respectively. The experimental study[20] has identified deuterium atom abstraction (DAA) from n-C_4D_{10} by $Ce_4O_9^-$ cluster that contains an $O_t^{-\bullet}$ radical. The estimated rate constant k_1($Ce_4O_9^-$+C_4D_{10}) is 3.7 × 10^{-11} cm^3 molecule^{-1} s^{-1}. Because of steric hindrance effect, the DAA by $Ce_5O_{11}^-$ that contains $O_b^{-\bullet}$ rather than $O_t^{-\bullet}$ is not happening or is much slower compared with the $Ce_4O_9^-$ system.

The experiment[20] suggests no evidence of DAA from n-C_4D_{10} by the $O_t^{-\bullet f}$-containing clusters CeO_3^-, $Ce_2O_5^-$, and $Ce_3O_7^-$ that have delocalized UPSDs. The *local spin effect* on C−H activation thus occurs in both $(Sc_2O_3)_{1,2}^+$ and $(CeO_2)_{1-4}O^-$ cluster systems. The DFT determined transition state energies for reactions 10 and 11 below are +0.07 and −0.07 eV with respect to the separated reactants, respectively:

$$Ce_3O_7^- + n\text{-}C_4H_{10} \rightarrow Ce_3O_7H^- + 2\text{-}C_4H_9 \qquad \Delta H_{0K} = -0.55\ \text{eV} \tag{10}$$

$$Ce_4O_9^- + n\text{-}C_4H_{10} \rightarrow Ce_4O_9H^- + 2\text{-}C_4H_9 \qquad \Delta H_{0K} = -0.74\ \text{eV} \tag{11}$$

As a result, reaction 10 is less favorable than reaction 11 both kinetically and thermodynamically.

One more example of *local spin effect* on C−H activation can be illustrated by studying the cerium oxide cluster cations. Figure S3, Supporting Information, shows that $(CeO_2)_{2-5}^+$ clusters ($\Delta = 1$) are $(OCeO)^\bullet$ heteroatom radicals, in which the UPSDs are distributed over one Ce and two O atoms in each system. The rates of HAA from methane by these clusters are thus relatively very slow. For example, $k_1(Ce_2O_4^+ + CH_4) = 2.2 \times 10^{-13}$ cm^3 molecule^{-1} s^{-1},[17] which is smaller than $k_1(M_2O_y^+ + CH_4)$ (M = Ti, Zr, Hf)[26] by more than 2 orders of magnitude. Note that the group 4 metal systems $Ti_2O_4^+$, $Zr_2O_4^+$, and $Hf_2O_4^+$ have highly localized UPSDs and contain highly reactive $O_t^{-\bullet}$ radicals.[16]

4.3. Oxide Clusters of Late Transition Metals. The search for HAA from methane, ethane, and butane by oxide cluster ions of late transition metals including iron and cobalt has also been carried out. So far, no evidence of HAA by $Fe_xO_y^\pm$ and $Co_xO_y^\pm$ ($x \geq 2$) clusters has been identified in our experiments. Normally the highest oxidation state of Fe is +3. One may expect that $(Fe_2O_3)_k^+$ clusters contain oxygen-centered radicals according to eq 3. The reaction of $Fe_2O_3^+$ with C_4H_{10} can be exothermic by DFT calculations:[29]

$$Fe_2O_3^+ + n\text{-}C_4H_{10} \rightarrow Fe_2O_3H^+ + 2\text{-}C_4H_9 \qquad \Delta H_{0K} = -0.69\ \text{eV} \tag{12}$$

The total UPSDs over the three oxygen atoms in $Fe_2O_3^+$ are very close to 1μ_B, while they are highly delocalized into the three oxygen atoms (0.37μ_B, 0.37μ_B, and 0.25μ_B, respectively), which can cause unfavorable kinetics in the reaction with C_4H_{10} according to the *local spin effect* illustrated for C−H activation by scandium and cerium oxide clusters.

4.4. Oxide Clusters of Main Group Elements. In addition to d- and f-block transition elements, C−H activation by $O^{-\bullet}$ radicals over oxide cluster cations of main group elements including Al, P, and so on has also been reported in literature.[13,30] For example, the HAA from methane under thermal collision conditions is observed over $(Al_2O_3)_{3-5}^+$ and $P_4O_{10}^+$. These clusters are all $\Delta = 1$ (eq 3), and DFT studies have confirmed existence of the $O_t^{-\bullet}$ radicals in $Al_8O_{12}^+$ and $P_4O_{10}^+$.[13] The identification of HAA by these main group species with $O^{-\bullet}$ centers further indicates that the oxygen-centered radicals rather than the d- or f-block metal atoms play the most important role in the C−H activation over related atomic clusters. It is noticeable that $Al_8O_{12}^+$ reacts much more slowly than $V_4O_{10}^+$ does with CH_4 [$k_1(Al_8O_{12}^+ + CH_4)/k_1(V_4O_{10}^+ + CH_4) = 0.0069$] although the enthalpies of reaction for HAA from CH_4 by these two clusters are very similar ($\Delta H_{0K} \approx -0.9$ eV).[13a,27]

5. C−H Activation over Heteronuclear Oxide Clusters

The metal oxide catalysts such as V_2O_5 are usually supported on Al_2O_3, SiO_2, and so on in practice. To further understand C−H activation by oxide clusters, we have studied reactions of methane, ethane, and butane with heteronuclear oxide clusters including V−Al, V−Si, V−P, and V−Y oxide cluster ions.[18,31−35] Note that eq 3 may be extended as eq 13 for heteronuclear oxide clusters $M^1_{x_1}M^2_{x_2}O_y^q$:

$$\Delta \equiv 2y - n_1x_1 - n_2x_2 + q \tag{13}$$

where n_i counts the highest oxidation state of M^i (i = 1 and 2).

The experiments have identified HAA from methane by $VAlO_4^+$, $V_3PO_{10}^+$, $V_2O_5(SiO_2)_{1-4}^+$, $(V_2O_5)_2SiO_2^+$, $V_3YO_9^+$, and $V_2Y_2O_8^+$ and HAA from ethane and (or) *n*-butane by $VAlO_5^-$, $V_{4-k}Al_kO_{11-k}^-$ (k = 1−3), $V_2O_6(SiO_2)_{1-4}^-$, $V_4O_{11}SiO_2^-$, VYO_4^+, and $VY_3O_7^+$. These are all $\Delta = 1$ clusters and contain $O_t^{-\bullet}$ or $O_t^{-\bullet f}$ radicals according to DFT calculations.[18,31−35] It is noticeable that the $O_t^{-\bullet}$ or $O_t^{-\bullet f}$ radicals are bonded with Al or Si atoms rather than V atoms in most of the V−Al or V−Si oxide clusters (Figure S4, Supporting Information). This suggests that for V_2O_5/SiO_2 and V_2O_5/Al_2O_3 catalysts in nanosize and further smaller regions or for related surface defect sites, the materials usually considered as support can participate directly in surface reactions, such as in the process of C−H activation.

All of the $V_{4-k}Y_kO_{10-k}^+$ (k = 0−3) clusters contain $O_t^{-\bullet}$ radicals that are bonded with V atoms and the V−$O_t^{-\bullet}$ bond length increases slightly as k increases (Figure S4, Supporting Information), which implies reactivity increase for HAA from CH_4 when k changes from 0 ($V_4O_{10}^+$) to 3 ($VY_3O_7^+$). However, the experiments (Figure 5) have identified significant reactivity decrease and barely observable HAA from CH_4 by $VY_3O_7^+$, although $VY_3O_7^+$ can readily react with ethane or butane to generate $VY_3O_7H^+$.[35] This puzzling result can be well rationalized if one defines local charges (Q_L) around the M−$O_t^{-\bullet}$ centers:

$$Q_L \equiv Q(M) + \sum_{i=1}^{N} Q(O_i)/f_i \tag{14}$$

where Q(M) and $Q(O_i)$ are charge population on element M (M = V for $V_{4-k}Y_kO_{10-k}^+$, k = 0−3) and the ith O atom that is directly bonded with M and f_i-fold coordinated in the cluster, respectively. Note that for $V_{4-k}Y_kO_{10-k}^+$ (k = 0−3) clusters, $N = 4$, $f_i = 1$ for $O_t^{-\bullet}$ and $f_i = 2$ for O_b. In the case that the widely used Mulliken population analysis (MPA) is adopted, the Q_L^{MPA} values of $V_{4-k}Y_kO_{10-k}^+$ are

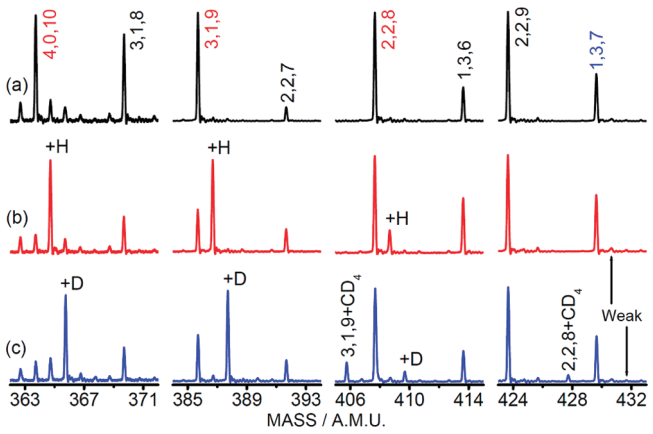

FIGURE 5. TOF mass spectra for reactions of $V_xY_yO_z^+$ (denoted as *x,y,z*) with He (a), about 0.4 Pa CH_4 (b), and about 0.4 Pa CD_4 (c).

0.38|e|, 0.23|e|, 0.11|e|, and 0.02|e| for $k = 0-3$, respectively. The Mulliken atomic charges may strongly depend on the choice of basis sets, while the results of natural population analysis (NPA) are stable with respect to basis set changes.[36] The natural charges Q_L^{NPA} of $V_{4-k}Y_kO_{10-k}^+$ are 0.31|e|, 0.07|e|, −0.17|e|, and −0.38|e| for $k = 0-3$, respectively. Both Q_L^{MPA} and Q_L^{NPA} are thus very well correlated with the cluster reactivity toward CH_4 (Figure 5).

The geometrically most favorable directions for CH_4 approaching the $O_t^{-\bullet}$ atoms in $V_{4-k}Y_kO_{10-k}^+$ ($k = 0-3$) clusters are around the $V-O_t^{-\bullet}$ bonds. The electrostatic potential (V) and its gradient (E_d) along the $V-O_t^{-\bullet}$ bonds in these clusters are shown in Figure 6. In terms of electrostatic interactions, an electron always sees attractive electric field ($E_d > 0$) when it approaches $V_4O_{10}^+$ and $V_3YO_9^+$ clusters along the $V-O_t^{-\bullet}$ direction. In contrast, an electron starts to see repulsive electric field ($E_d < 0$) at $d(O_t^{-\bullet}-e^-)$ around 350 and 250 pm when it approaches $VY_3O_7^+$ and $V_2Y_2O_8^+$ clusters, respectively. The HAA by $O_t^{-\bullet}$ over the atomic clusters as shown in Figure 4 is primarily characterized with ET. As a result, it is reasonable to find that $V_2Y_2O_8^+$ is much less reactive than $V_4O_{10}^+$ and $V_3YO_9^+$ and the reactivity of $VY_3O_7^+$ is barely observable in the reaction with CH_4 (Figure 5).

The above *local charge effect* realized for the $V_{4-k}Y_kO_{10-k}^+$ ($k = 0-3$) system can also be used to interpret the reactivity decrease of $V_2O_5(SiO_2)_k^+$ ($k = 1-4$) as increase of the cluster size and the relatively very low reactivity of $Al_8O_{12}^+$ toward CH_4 (Figure 7). These clusters have a net charge of +1|e| while Q_L^{NPA} ranges from −0.38|e| ($VY_3O_7^+$) to 0.96|e| ($V_2SiO_7^+$). The *anisotropic distribution of the charge within the small atomic clusters* can influence the reactivity toward methane dramatically. The larger and more positive Q_L

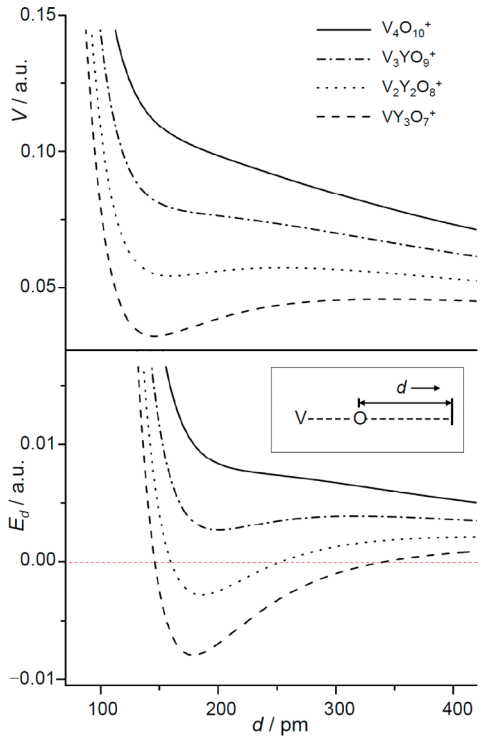

FIGURE 6. Electrostatic potential (V) and its gradient (E_d) along the $V-O_t^{-\bullet}$ bonds in $V_{4-k}Y_kO_{10-k}^+$ ($k = 0-3$) clusters. The cluster structures are given in Figure S4, Supporting Information.

value around $O^{-\bullet}$ center generally corresponds to higher reactivity, which is also in line with the result that $O^{-\bullet}$-containing cationic clusters are much more reactive than the corresponding anionic ones because the Q_L value of an anion is usually negative due to the presence of the net charge.

The local spin and local charge effects on C–H activation have been demonstrated. These two effects may not be completely independent because an $O^{-\bullet}$ radical (singly charged, with UPSD) usually has less negative charges than an O^{2-} ion (doubly charged, without UPSDs) does. For example, the natural charges on the $O_t^{-\bullet}$ and O_t^{2-} atoms in $V_4O_{10}^+$ are −0.018|e| and −0.112|e|, respectively. This means that high HAA reactivity of the $O^{-\bullet}$ radicals over the O^{2-} ions can be partly due to the less negative (or more positive) local charges of the former over the latter. Mayer has recently suggested that *the presence of unpaired spin density at the abstracting atom is not a requirement for, or a predictor of, HAT reactivity* (HAT = hydrogen atom transfer).[24] We thus propose that HAA from alkanes by an O^{2-} ion can be promoted by supplying more positive charges around the abstracting center. Figure 8 indicates that the DFT calculated energy barrier for methane activation by O_t^{2-} ions ($V^{5+}=O_t^{2-}$) in the neutral V_4O_{10} cluster is very high ($\Delta H_{0K} = 1.38$ eV at

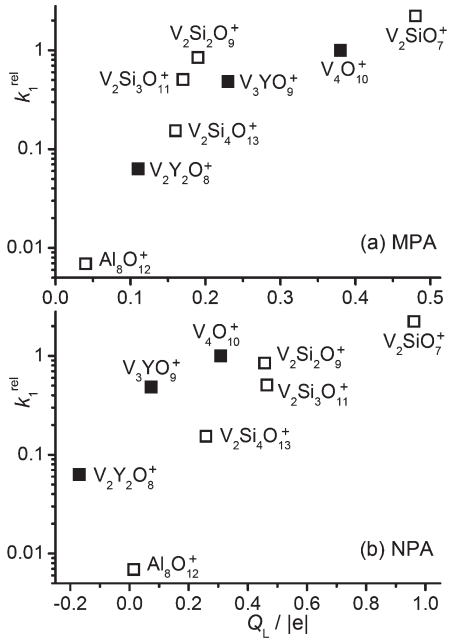

FIGURE 7. Variation of the experimentally determined reaction rate constants (k_1^{rel})[13a,18,27,35] with respect to the local charges (Q_L) from Mulliken (a) and natural population analysis (b), where $k_1^{rel} = k_1$-(X+CH_4)/k_1($V_4O_{10}^+$+CH_4) and X = $Al_8O_{12}^+$, $V_2O_5(SiO_2)_{1-4}^+$, and $V_{4-k}Y_kO_{10-k}^+$ (k = 0–2).

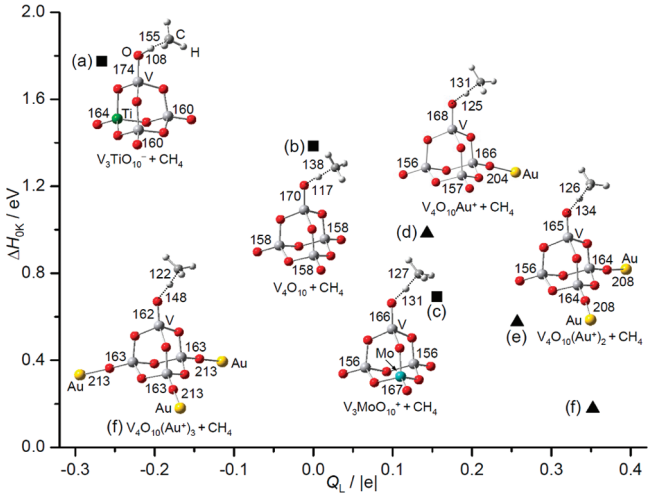

FIGURE 8. B3LYP/TZVP/SDD calculated structures and energetics for hydrogen atom abstraction from methane by the V^{5+}=O_t^{2-} centers in V_4O_{10}, $V_3TiO_{10}^-$, $V_3MoO_{10}^+$, and $V_4O_{10}(Au^+)_{1-3}$ model clusters. The transition state structures are given.

Q_L^{NPA} = 0|e|), while upon doping Mo^{6+} into V_4O_{10}, which increases Q_L^{NPA} to 0.16|e|, the barrier can be significantly decreased (ΔH_{0K} = 0.69 eV). The local charges around V^{5+}=O_t^{2-} centers can also be supplied by positively charged gold atoms [Q_L^{NPA} = 0.14|e|, 0.16|e|, and 0.35|e| for Au^+, $(Au^+)_2$, and $(Au^+)_3$ systems, respectively]. We speculate that these gold atoms may be considered as gold anodes in practice. The local charge effect on C–H activation in catalysis and electrocatalysis[37] for condensed phase systems may be studied in the future.

6. Concluding Remarks

Homonuclear and heteronuclear oxide clusters that are the least oxygen-rich (Δ = 1, eqs 3 and 13) usually contain oxygen-centered radicals ($O^{-\bullet}$). The $O^{-\bullet}$ radicals can be exclusively bonded with main group elements rather than transition metal atoms in some heteronuclear oxide clusters such as $V_2O_5(SiO_2)_{1-4}^+$ and $V_2O_6(SiO_2)_{1-4}^-$. The more oxygen-rich ($\Delta > 1$) clusters with specific compositions can also contain the $O^{-\bullet}$ radicals or even $O^{-\bullet}$ biradicals. Hydrogen atom abstraction from methane and other alkanes by the $O^{-\bullet}$ radicals over atomic clusters are usually exothermic, while the rates of reactions or the reactivity of the clusters heavily depends on the geometric and electronic structures as well as the charge environments involved with the $O^{-\bullet}$ radicals. The $O^{-\bullet}$-containing clusters with highly localized unpaired spin densities are usually much more reactive than the ones with delocalized unpaired spin densities (*local spin effect*). The $O^{-\bullet}$-containing cations are generally much more reactive than the corresponding anions. The local charge distributions around the $O^{-\bullet}$ centers in the clusters such as $V_{4-k}Y_kO_{10-k}^+$ (k = 0–3) and $V_2O_5(SiO_2)_{1-4}^+$ vary largely and control the large variation of the cluster reactivity toward methane (*local charge effect*). The study of the atomic clusters, the intermediate state of matter, has revealed rather detailed structure–property relationships involved with C–H activation by oxygen-centered radicals. Oxide clusters with larger sizes and heteronuclear oxide clusters involving both early and late transition metals or both d- and f-block metals may be studied in the future to further understand the C–H activation. Spin and charge can be readily controllable physical quantities. Their impact on C–H activation demonstrated can be a good clue for rational design of catalysts for alkane transformation in practice.

This work is supported by Chinese Academy of Sciences (Knowledge Innovation Program KJCX2-EW-H01, Hundred Talents Fund), the National Natural Science Foundation of China (Nos. 20803083 and 20933008), and Major Research Plan of China (No. 2011CB932302).

Supporting Information. Collection and comparison of DFT calculated cluster structures and charge population analysis on reactions 1 and 7. This material is available free of charge via the Internet at http://pubs.acs.org.

BIOGRAPHICAL INFORMATION

Xun-Lei Ding received his B.S. degree in physics in 1999 and Ph. D. degree in chemistry in 2004 from University of Science and Technology of China (USTC). After postdoctoral stays with Prof. Jian-Guo Hou at USTC and Prof. Maria Peressi at CNR-INFM DEMOCRITOS (Italy), he joined Institute of Chemistry, Chinese Academy of Sciences (ICCAS), in 2007. His research interests include first principle studies on structural and reactivity properties of clusters and surfaces.

Xiao-Nan Wu received his B.S. degree in chemistry from Beijing University of Chemical Technology in 2007 and is currently a Ph.D. candidate with Sheng-Gui He.

Yan-Xia Zhao received her B.S. degree in chemistry from Shanxi Normal University in 2005, M.S. degree in chemistry from Beijing Normal University in 2008, and Ph.D. degree in chemistry from ICCAS in 2011.

Sheng-Gui He received his B.S. degree in physics in 1997 and Ph.D. degree in chemistry in 2002 from USTC. After postdoctoral stays with Prof. Dennis J. Clouthier at University of Kentucky and Prof. Elliot R. Bernstein at Colorado State University, he joined ICCAS in 2007. His research interests are experimental and theoretical studies of reactive intermediates including free radicals and atomic clusters.

FOOTNOTES

*To whom correspondence should be addressed. E-mail: shengguihe@iccas.ac.cn.

REFERENCES

1 Labinger, J. A.; Bercaw, J. E. Understanding and Exploiting C−H Bond Activation. *Nature* **2002**, *417*, 507–514.

2 Wang, G.-J.; Zhou, M.-F. Probing the Intermediates in the $MO+CH_4 \leftrightarrow M+CH_3OH$ Reactions by Matrix Isolation Infrared Spectroscopy. *Int. Rev. Phys. Chem.* **2008**, *27*, 1–25.

3 Schlangen, M.; Schwarz, H. Ligand and Electronic-Structure Effects in Metal-Mediated Gas-Phase Activation of Methane: A Cold Approach to a Hot Problem. *Dalton Trans.* **2009**, 10155–10165.

4 Roithová, J.; Schröder, D. Selective Activation of Alkanes by Gas-Phase Metal Ions. *Chem. Rev.* **2010**, *110*, 1170–1211.

5 Balcells, D.; Clot, E.; Eisenstein, O. C−H Bond Activation in Transition Metal Species from a Computational Perspective. *Chem. Rev.* **2010**, *110*, 749–823.

6 Fokin, A. A.; Schreiner, P. R. Selective Alkane Transformations via Radicals and Radical Cations: Insights into the Activation Step from Experiment and Theory. *Chem. Rev.* **2002**, *102*, 1551–1593.

7 Viggiano, A. A.; Morris, R. A.; Miller, T. M.; Friedman, J. F.; MenedezBarreto, M.; Paulson, J. F.; Michels, H. H.; Hobbs, R. H.; Montgomery, J. A. Reaction on the $O^- + CH_4$ Potential Energy Surface: Dependence on Translational and Internal Energy and on Isotopic Composition, 93−1313 K. *J. Chem. Phys.* **1997**, *106*, 8455–8463.

8 Liu, H.-F.; Liu, R.-S.; Liew, K. Y.; Johnson, R. E.; Lunsford, J. H. Partial Oxidation of Methane by Nitrous-Oxide over Molybdenum on Silica. *J. Am. Chem. Soc.* **1984**, *106*, 4117–4121.

9 Launay, H.; Loridant, S.; Nguyen, D. L.; Volodin, A. M.; Dubois, J. L.; Millet, J. M. M. Vanadium Species in New Catalysts for the Selective Oxidation of Methane to Formaldehyde: Activation of the Catalytic Sites. *Catal. Today* **2007**, *128*, 176–182.

10 Chiesa, M.; Giamello, E.; Che, M. EPR Characterization and Reactivity of Surface-Localized Inorganic Radicals and Radical Ions. *Chem. Rev.* **2010**, *110*, 1320–1347.

11 Castleman, A. W., Jr.; Keesee, R. G. Clusters: Bridging the Gas and Condensed Phases. *Acc. Chem. Res.* **1986**, *19*, 413–419.

12 (a) Justes, D. R.; Mitrić, R.; Moore, N. A.; Bonačić-Koutecký, V.; Castleman, A. W., Jr. Theoretical and Experimental Consideration of the Reactions between $V_xO_y^+$ and Ethylene. *J. Am. Chem. Soc.* **2003**, *125*, 6289–6299. (b) Tyo, E. C.; Nőbler, M.; Mitrić, R.; Bonačić-Koutecký, V.; Castleman, A. W., Jr. Reactivity of Stoichiometric Titanium Oxide Cations. *Phys. Chem. Chem. Phys.* **2011**, *13*, 4243–4249 and references therein.

13 (a) Feyel, S.; Döbler, J.; Hoeckendorf, R.; Beyer, M. K.; Sauer, J.; Schwarz, H. Activation of Methane by Oligomeric $(Al_2O_3)_x^+$ (x = 3,4,5): The Role of Oxygen-Centered Radicals in Thermal Hydrogen-Atom Abstraction. *Angew. Chem., Int. Ed.* **2008**, *47*, 1946–1950. (b) Dietl, N.; Engeser, M.; Schwarz, H. Room-Temperature C−H Bond Activation of Methane by Bare $[P_4O_{10}]^{\bullet+}$. *Angew. Chem., Int. Ed.* **2009**, *48*, 4861–4863.

14 Dong, F.; Heinbuch, S.; Xie, Y.; Rocca, J. J.; Bernstein, E. R.; Wang, Z. C.; Deng, K.; He, S. G. Experimental and Theoretical Study of the Reactions between Neutral Vanadium Oxide Clusters and Ethane, Ethylene, and Acetylene. *J. Am. Chem. Soc.* **2008**, *130*, 1932–1943.

15 Zhai, H.-J.; Zhang, X.-H.; Chen, W.-J.; Huang, X.; Wang, L.-S. Stoichiometric and Oxygen-Rich $M_2O_n^-$ and M_2O_n (M = Nb, Ta; n = 5−7) Clusters: Molecular Models for Oxygen Radicals, Diradicals, and Superoxides. *J. Am. Chem. Soc.* **2011**, *133*, 3085–3094.

16 Zhao, Y.-X.; Ding, X.-L.; Ma, Y.-P.; Wang, Z.-C.; He, S.-G. Transition Metal Oxide Clusters with Character of Oxygen-Centered Radical: A DFT Study. *Theor. Chem. Acc.* **2010**, *127*, 449–465.

17 Wu, X.-N.; Zhao, Y.-X.; Xue, W.; Wang, Z.-C.; He, S.-G.; Ding, X.-L. Active Sites of Stoichiometric Cerium Oxide Cations $(Ce_mO_{2m}^+)$ Probed by Reactions with Carbon Monoxide and Small Hydrocarbon Molecules. *Phys. Chem. Chem. Phys.* **2010**, *12*, 3984–3997.

18 Ding, X.-L.; Zhao, Y.-X.; Wu, X.-N.; Wang, Z.-C.; Ma, J.-B.; He, S.-G. Hydrogen-Atom Abstraction from Methane by Stoichiometric Vanadium-Silicon Heteronuclear Oxide Cluster Cations. *Chem.—Eur. J.* **2010**, *16*, 11463–11470.

19 Zhao, Y.-X.; Yuan, J.-Y.; Ding, X.-L.; He, S.-G.; Zheng, W.-J. Electronic Structure and Reactivity of a Biradical Cluster: $Sc_3O_6^-$. *Phys. Chem. Chem. Phys.* **2011**, *13*, 10084–10090.

20 Wu, X.-N.; Ding, X.-L.; Bai, S.-M.; Xu, B.; He, S.-G.; Shi, Q. Experimental and Theoretical Study of the Reactions between Cerium Oxide Cluster Anions and Carbon Monoxide: Size-Dependent Reactivity of $Ce_nO_{2n+1}^-$ (n = 1−21). *J. Phys. Chem. C.* **2011**, *115*, 13329–13337.

21 Che, M.; Tench, A. J. Characterization and Reactivity of Mononuclear Oxygen Species on Oxide Surfaces. *Adv. Catal.* **1982**, *31*, 77–133.

22 Xu, B.; Zhao, Y.-X.; Li, X.-N.; Ding, X.-L.; He, S.-G. Experimental and Theoretical Study of Hydrogen Atom Abstraction from n-Butane by Lanthanum Oxide Cluster Anions. *J. Phys. Chem. A* **2011**, *115*, 10245–10250.

23 Ma, J.-B.; Wu, X.-N.; Zhao, Y.-X.; Ding, X.-L.; He, S.-G. Characterization of Mononuclear Oxygen-Centered Radical ($O^{-\bullet}$) in $Zr_2O_8^-$ Cluster. *J. Phys. Chem. A* **2010**, *114*, 10024–10027.

24 Mayer, J. M. Understanding Hydrogen Atom Transfer: From Bond Strengths to Marcus Theory. *Acc. Chem. Res.* **2011**, *44*, 36–46.

25 Schwarz, H. Chemistry with Methane: Concepts Rather than Recipes. *Angew. Chem., Int. Ed.* **2011**, *50*, 10096–10115.

26 Zhao, Y.-X.; Wu, X.-N.; Wang, Z.-C.; He, S.-G.; Ding, X.-L. Hydrogen-Atom Abstraction from Methane by Stoichiometric Early Transition Metal Oxide Cluster Cations. *Chem. Commun.* **2010**, *46*, 1736–1738.

27 Feyel, S.; Döbler, J.; Schröder, D.; Sauer, J.; Schwarz, H. Thermal Activation of Methane by Tetranuclear $V_4O_{10}^+$. *Angew. Chem., Int. Ed.* **2006**, *45*, 4681–4685.

28 Dietl, N.; van der Linde, C.; Schlangen, M.; Beyer, M. K.; Schwarz, H. Diatomic $[CuO]^+$ and Its Role in the Spin-Selective Hydrogen- and Oxygen-Atom Transfers in the Thermal Activation of Methane. *Angew. Chem., Int. Ed.* **2011**, *50*, 4966–4969.

29 Xue, W.; Yin, S.; Ding, X.-L.; He, S.-G.; Ge, M.-F. Ground State Structures of $Fe_2O_{4-6}^+$ Clusters Probed by Reactions with N_2. *J. Phys. Chem. A* **2009**, *113*, 5302–5309.

30 de Petris, G.; Troiani, A.; Rosi, M.; Angelini, G.; Ursini, O. Methane Activation by Metal-Free Radical Cations: Experimental Insight into the Reaction Intermediate. *Chem.—Eur. J.* **2009**, *15*, 4248–4252.

31 Wang, Z.-C.; Wu, X.-N.; Zhao, Y.-X.; Ma, J.-B.; Ding, X.-L.; He, S.-G. Room-Temperature Methane Activation by a Bimetallic Oxide Cluster $AlVO_4^+$. *Chem. Phys. Lett.* **2010**, *489*, 25–29.

32 Ma, J.-B.; Wu, X.-N.; Zhao, X.-X.; Ding, X.-L.; He, S.-G. Methane Activation by $V_3PO_{10}^{\bullet+}$ and $V_4O_{10}^{\bullet+}$ Clusters: A Comparative Study. *Phys. Chem. Chem. Phys.* **2010**, *12*, 12223–12228.

33 Zhao, Y.-X.; Wu, X.-N.; Ma, J.-B.; He, S.-G.; Ding, X.-L. Experimental and Theoretical Study of the Reactions between Vanadium-Silicon Heteronuclear Oxide Cluster Anions with n-Butane. *J. Phys. Chem. C* **2010**, *114*, 12271–12279.

34 Wang, Z.-C.; Wu, X.-N.; Zhao, Y.-X.; Ma, J.-B.; Ding, X.-L.; He, S.-G. C−H Activation on Aluminum-Vanadium Bimetallic Oxide Cluster Anions. *Chem.—Eur. J.* **2011**, *17*, 3449–3457.

35 Li, Z.-Y.; Zhao, Y.-X.; Wu, X.-N.; Ding, X.-L.; He, S.-G. Methane Activation by Yttrium-Doped Vanadium Oxide Cluster Cations: Local Charge Effects. *Chem.—Eur. J.* **2011**, *17*, 11728–11733.

36 Reed, A. E.; Weinstock, R. B.; Weinhold, F. Natural Population Analysis. *J. Chem. Phys.* **1985**, *83*, 735–746.

37 Kulakovskaya, S. I.; Kulikov, A. V.; Berdnikov, V. M.; Ioffe, N. T.; Shestakov, A. F. Electrochemical and ESR Study of the C−H Bond Activation. Electrocatalytical Oxidation with Participation of Radical Cation of Phenazine-di-N-Oxide. *Electrochim. Acta* **2002**, *47*, 4245–4254.